ISSN 1674-1056
http://cpb.iphy.ac.cn
http://iopscience.iop.org/cpb
中国物理 B
Chinese Physics
中国物理
Chinese Physics B

Head-on collision between two solitary waves in one-dimensional bead chain

Fu-Gang Wang(王扶刚), Yang-Yang Yang(杨阳阳), Juan-Fang Han(韩娟芳), Wen-Shan Duan(段文山)
Citation: Chin. Phys. B . 2018, 27(4): 044501. **doi:** 10.1088/1674-1056/27/4/044501

Journal homepage: http://cpb.iphy.ac.cn; http://iopscience.iop.org/cpb

What follows is a list of articles you may be interested in

A new four-dimensional chaotic system with first Lyapunov exponent ≈ 22, hyperbolic curve and circular paraboloid types of equilibria and its switching synchronization by an adaptive global integral sliding mode control

Jay Prakash Singh, Binoy Krishna Roy, Zhouchao Wei(魏周超)
Chin. Phys. B . 2018, 27(4): 040503. **doi:** 10.1088/1674-1056/27/4/040503

Effects of intrinsic and extrinsic noises on transposons kinetics

Alssadig A M Yousif, Lulu Lu(鹿露露), Mengyan Ge(葛梦炎), Ying Xu(徐莹), Ya Jia(贾亚)
Chin. Phys. B . 2018, 27(3): 030501. **doi:** 10.1088/1674-1056/27/3/030501

Generalized Chaplygin equations for nonholonomic systems on time scales

Shi-Xin Jin(金世欣), Yi Zhang(张毅)
Chin. Phys. B . 2018, 27(2): 020502. **doi:** 10.1088/1674-1056/27/2/020502

Envelope solitary waves and their reflection and transmission due to impurities in a granular material

Wen-Qing Du(杜文青), Jian-An Sun(孙建安), Yang-Yang Yang(杨阳阳), Wen-Shan Duan(段文山)
Chin. Phys. B . 2018, 27(1): 014501. **doi:** 10.1088/1674-1056/27/1/014501

A necessary and sufficient condition for transforming autonomous systems into linear autonomous Birkhoffian systems

Cui Jin-Chao, Liu Shi-Xing, Song Duan
Chin. Phys. B . 2013, 22(10): 104501. **doi:** 10.1088/1674-1056/22/10/104501

Head-on collision between two solitary waves in a one-dimensional bead chain*

Fu-Gang Wang(王扶刚)[1], Yang-Yang Yang(杨阳阳)[1], Juan-Fang Han(韩娟芳)[1,2], and Wen-Shan Duan(段文山)[1,2,†]

[1] *Institute of Modern Physics & College of Physics and Electronic Engineering and Joint Laboratory of Atomic and Molecular Physics of Northwest Normal University, Lanzhou* 730070, *China*

[2] *Institute of Modern Physics, Chinese Academy of Sciences, Lanzhou* 730000, *China*

(Received 24 November 2017; revised manuscript received 12 January 2018; published online 10 March 2018)

The head on collision between two opposite propagating solitary waves is studied in the present paper both numerically and analytically. The interesting result is that no phase shift is observed which is different from that found in other branches of physics. It is found that the maximum amplitude in the process of the head on collision is close to the linear sum of two colliding solitary waves.

Keywords: discrete system, bead chain, solitary waves

PACS: 45.05.+x, 05.45.–a, 45.70.–n **DOI:** 10.1088/1674-1056/27/4/044501

1. Introduction

The solitary waves were found by Scott Rusell in 1834. Later, the KdV equation was obtained in 1895.[1] An extraordinary series of events happened around 1965 when Kruskal and Zabusky discovered a pulse-like solitary wave solution of the KdV equation,[2] for which the name "soliton" was proposed. However, the presence of solitary waves in the bead chain was first discovered and studied by Nesterenko *et al.*[3] in 1984. It indicated that the interaction between spheres obeyed the Hertzian law, and the interaction forces with a form of solitary waves propagated in the bead chain. Later, Coste *et al.*[4] experimentally studied the relationship between the propagation velocity of the isolated wave and the maximum amplitude and static force. In the pioneering work of Nesterenko,[3,5,6] wave propagation in a 1D assembly of beads has a rich content in physics due to the nonlinear nature of the interaction between spheres. The most commonly used method of the study of this nonlinear wave is the Poincare–Lighthill–Kuo (PLK) method,[7–9] which has been extensively used in many branches of physics, such as in plasma physics,[10,11] in Boes–Einstein condensates,[9,12] in nonlinear lattice dynamics,[13,14] etc.

The excitation, propagation, and interaction of solitary waves are important issues in theoretical studies. Recently several studies have reported, both experimentally and numerically, a large number of phenomena associated with this type of wave in Hertzian linear chains, ranging from solitary wave interaction with boundaries[4,15–17] and wave mitigation in tapered chains[18–21] to energy localization in chains with mass defects[22–24] and pulse reflection and transmission due to impurities in a granular chain.[25–27] With the further reports on solitary wave correlation studies, the problem of interaction between solitary waves has attracted rapidly growing interest because of the significance of understanding the dynamics of granular matter. For instance, the authors in Ref. [28] studied the interaction between the solitary waves in the Toda lattice. It shows that the Toda lattice enables capturing both copropagating and counterpropagating soliton collisions and the existence of phase shift after collision. The interaction between the solitary waves in the plasma[29–34] has been widely reported, it is the well-known feature of the presence of phase shifts as a result of the solitonic collisions in the plasma. However, the interaction of solitary waves in granular chains is little understood. Francisco Santibanez *et al.*[35] studied only experimentally the interaction between two solitary waves that approach one another in a linear chain of spheres interacting via the Hertz potential. When these counterpropagating waves collide, they cross each other and a phase shift in respect to the noninteracting waves is introduced as a result of the nonlinear interaction potential. As a result, in the literature, one refers to these waves as solitary waves. Two opposite propagating solitary waves can pass through each other without suffering any interaction except for a slight shift in their positions compared to where they would have been had they not passed through one another. In this letter, by using the reductive perturbation method, we obtain a pair of KdV solitary waves described by uncoupled KdV equations, one moving rightward and the other moving leftward, to capture the evolution of general initial data, it is used to study the interaction of solitary waves in a 1D granular medium. The head on collision between two

*Project supported by the National Magnetic Confinement Fusion Science Program of China (Grant No. 2014GB104002), the National Natural Science Foundation of China (Grant No. 11647313), the Youth Science and Technology Foundation of Gansu Province, China (Grant No. 1606RJYA263), and the Institutes of Higher Education Institutions of Gansu Province, China (Grant No. 2015B-022).

†Corresponding author. E-mail: duanws@nwnu.edu.cn

© 2018 Chinese Physical Society and IOP Publishing Ltd

opposite propagating solitary waves is studied in the present study. The interesting result is that no phase shift is observed. It is found that the maximum amplitude in the process of the head on collision is close to the linear sum of two colliding solitary waves.

This paper is organized as follows. In Section 2 we set up the model. In Section 3 we give the numerical results. Finally, in Section 4 the conclusion is given in the last section.

2. Physical model

We consider an alignment of N identical elastic spheres, each of mass m and radius R, placed in such a way that they are barely in contact with each other. There is no grain-grain interaction when there is no contact, but when an external perturbation is applied to the system initially, different pulses may be evolved into the system. In this process, the elastic deformations are accompanied. Under elastic deformation, the energy stored at the contact between two elastic beads under compression with the Hertz potential is $U=(2/5)k\delta^{5/2}$, where δ is the overlap deformation between beads and $k=(R/2)^{1/2}/D(Y,\sigma)$, $D(Y,\sigma)=(3/2)[(1-\sigma^2)/Y]$, R is the bead radius, Y is the Young modulus, and σ is the Poisson ratio of the bead material. The dynamics of the bead chain is described by the N coupled nonlinear equations,

$$m_i\frac{\mathrm{d}^2u_i}{\mathrm{d}t^2}=nk[(2R+u_{i-1}-u_i)^{n-1}-(2R+u_i-u_{i+1})^{n-1}] \quad (1)$$

with $i=1,2,\ldots,N$, where m_i is the bead mass, $u_i=(2i-1)R+s_i$ denotes the absolute position of bead i, and s_i is the displacement from its equilibrium position of bead i. In general, the magnitude of n depends upon the contact geometry between the beads and typically varies between $n=5/2$ and 3,[36,37] and in our work $n=5/2$. If there is great enough prestress, the bead radius will be $R'=R-\delta_0/2$, δ_0 is the initial overlap deformation between two beads. In the continuous long-wavelength limit, and $\delta_0\gg s_i-s_{i+1}$, equation (1) becomes[27,39–41]

$$\frac{\mathrm{d}^2s}{\mathrm{d}t^2}=B_1\left(\frac{\mathrm{d}^2s}{\mathrm{d}i^2}+\frac{1}{12}\frac{\mathrm{d}^4s}{\mathrm{d}i^4}\right)+B_2\frac{\mathrm{d}^2s}{\mathrm{d}i^2}, \quad (2)$$

where

$$B_1=\frac{n(n-1)k\delta_0^{n-2}}{m_i},$$
$$B_2=-\frac{n(n-1)(n-2)k\delta_0^{n-3}}{m_i}, \quad s_i(t)=s(i,t),$$

and i is assumed to be a continuous variable.

Now we study the interaction of a pair of uncoupled KdV solitary waves in a 1D granular chain, as is shown in Fig. 1. We place a chain of N same beads from $i=1$ to $i=N$. We assume that there are two opposite propagating KdV solitary waves labeled by L and R, respectively. One is propagating from the left to the right direction and the other is in the negative direction. Initially, both KdV solitary waves are far apart. After some time, they interact, collide, and then depart. In general, after the collision, there is a phase shift of both solitary waves.[28–35]

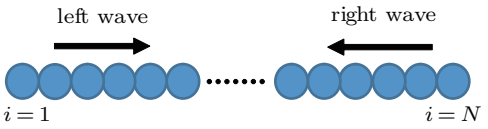


Fig. 1. (color online) Head-on collision of two KdV solitary waves in a one dimensional bead chain.

According to the reductive perturbation method,[7–9,30,38,39] we introduce the stretched coordinates in the region $i>0$:

$$\xi=\varepsilon(k_{\mathrm{L}}x-\lambda_{\mathrm{L}}t+\varepsilon^2P(\eta,\tau)+\cdots,$$
$$\eta=\varepsilon(k_{\mathrm{R}}x-\lambda_{\mathrm{R}}t+\varepsilon^2Q(\xi,\tau)+\cdots,$$
$$\tau=\varepsilon^3i,$$

where ξ and η denote the trajectories of two solitary waves traveling in two different directions, respectively. λ_{L} and λ_{R} are the two corresponding propagation speeds. ε is a small parameter ($\varepsilon\ll1$).[30] The dependent variables are expanded around the equilibrium values in power of ε:

$$s=\varepsilon s_1+\varepsilon^3s_2+\cdots, \quad s=s(\xi,\eta,\tau).$$

Substituting these expansions into Eq. (2) and collecting terms in different powers of ε, at the lowest order we obtain $\lambda_{\mathrm{L}}=k_{\mathrm{L}}\sqrt{B_1}$, $\lambda_{\mathrm{R}}=k_{\mathrm{R}}\sqrt{B_1}$. Then we have $s_1=s^{\mathrm{L}}(\xi,\tau)+s^{\mathrm{R}}(\eta,\tau)$. s^{L} and s^{R} satisfy the KdV equations respectively.

$$\frac{\partial s^{\mathrm{L}}}{\partial\tau}+\alpha^{\mathrm{L}}s^{\mathrm{L}}\frac{\partial s^{\mathrm{L}}}{\partial\xi}+\beta^{\mathrm{L}}\frac{\partial^3s^{\mathrm{L}}}{\partial\xi^3}=0, \quad (3)$$
$$\frac{\partial s^{\mathrm{R}}}{\partial\tau}+\alpha^{\mathrm{R}}s^{\mathrm{R}}\frac{\partial s^{\mathrm{R}}}{\partial\eta}+\beta^{\mathrm{R}}\frac{\partial^3s^{\mathrm{R}}}{\partial\eta^3}=0, \quad (4)$$

where $\alpha^{\mathrm{L}}=B_2k_{\mathrm{L}}^2/2B_1$, $\beta^{\mathrm{L}}=k_{\mathrm{L}}^3/24$, and $\alpha^{\mathrm{R}}=B_2k_{\mathrm{R}}^2/2B_1$, $\beta^{\mathrm{R}}=k_{\mathrm{R}}^3/24$, one of the simple solutions of the KdV equation can be written as

$$v^{\mathrm{L}}=v_m^{\mathrm{L}}\,\mathrm{sech}^2\frac{\xi-u_0^{\mathrm{L}}\tau}{D^{\mathrm{L}}}, \quad (5)$$
$$v^{\mathrm{R}}=v_m^{\mathrm{R}}\,\mathrm{sech}^2\frac{\eta-u_0^{\mathrm{R}}\tau}{D^{\mathrm{R}}}, \quad (6)$$

where $v_m^{\mathrm{L}}=3u_0^{\mathrm{L}}/\alpha^{\mathrm{L}}$, $D^{\mathrm{L}}=2\sqrt{\beta^{\mathrm{L}}/u_0^{\mathrm{L}}}$, and $v_m^{\mathrm{R}}=3u_0^{\mathrm{R}}/\alpha^{\mathrm{R}}$, $D^{\mathrm{R}}=2\sqrt{\beta^{\mathrm{R}}/u_0^{\mathrm{R}}}$, u_0^{L} and u_0^{R} are modulational parameters which can adjust the wave amplitude. All the physical quantities are dimensionless. The length, the velocity, and the mass are normalized by the diameter of a bead, the acoustic velocity of the system, and the mass of a bead. In this dimensionless system, the unit time is $\tau_0=3.737\times10^{-7}$ s, the unit length is $L_0=0.0002$ m, and the unit mass is $m_0=1.0472\times10^{-5}$ kg.

Then, in the experimental coordinate we can obtain the displacement and the velocity of each bead, which can be described as a kink solution and a solitary wave solution in the system:

$$s^{\mathrm{L}} = s_m^{\mathrm{L}} \tanh\left[\sqrt{\frac{6u_0^{\mathrm{L}}}{k_{\mathrm{L}}^3}}(\xi - u_0^{\mathrm{L}}\tau)\right], \tag{7}$$

$$v^{\mathrm{L}} = v_m^{\mathrm{L}} \operatorname{sech}^2\left[\sqrt{\frac{6u_0^{\mathrm{L}}}{k_{\mathrm{L}}^3}}(\xi - u_0^{\mathrm{L}}\tau)\right], \tag{8}$$

$$s^{\mathrm{R}} = s_m^{\mathrm{R}} \tanh\left[\sqrt{\frac{6u_0^{\mathrm{R}}}{k_{\mathrm{R}}^3}}(\eta - u_0^{\mathrm{R}}\tau)\right], \tag{9}$$

$$v^{\mathrm{R}} = v_m^{\mathrm{R}} \operatorname{sech}^2\left[\sqrt{\frac{6u_0^{\mathrm{R}}}{k_{\mathrm{R}}^3}}(\eta - u_0^{\mathrm{R}}\tau)\right], \tag{10}$$

where $s_m^{\mathrm{L}} = B_1\sqrt{6u_0^{\mathrm{L}}k_{\mathrm{L}}}/B_2k_{\mathrm{L}}$, $v_m^{\mathrm{L}} = 6B_1u_0^{\mathrm{L}}/B_2k_{\mathrm{L}}^2$, and $s_m^{\mathrm{R}} = B_1\sqrt{6u_0^{\mathrm{R}}k_{\mathrm{R}}}/B_2k_{\mathrm{R}}$, $v_m^{\mathrm{R}} = 6B_1u_0^{\mathrm{R}}/B_2k_{\mathrm{R}}^2$. It is well known that the above solutions of the KdV equation are exactly reliable in a 1D granular system and the relevant numerical results have already been carried out, as shown in Ref. [27].

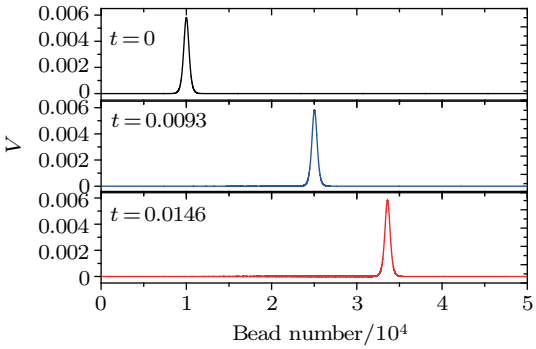


Fig. 2. (color online) Simulation results of the evolution of a KdV solitary wave at different times.

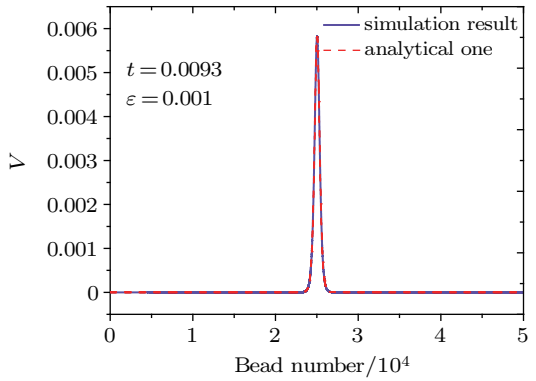


Fig. 3. (color online) The comparisons between simulation results and the analytical ones with the same initial conditions at $t = 0.0093$. In the figure, the red dotted line represents the analytical solution and the blue solid line represents the simulated results.

3. Numerical results and discussion

We choose a 1D chain consisting of the same 5×10^4 beads. The relevant parameters of the beads are as follows: Young's modulus $Y = 2 \times 10^{11}$ Pa, Poisson's ratio $\sigma = 0.3$, the density $\rho = 7.78 \times 10^3$ kg/m^3, radius $R = 0.001$ m, and the initial overlap $\delta = 0.0003$ m. The initial conditions of the displacements from their equilibrium positions and the corresponding velocities of all beads are chosen from the analytical results, Eqs. (7), (8) and Eqs. (9), (10), where $u_0^{\mathrm{L}} = u_0^{\mathrm{R}} = 1$, $k_{\mathrm{L}} = k_{\mathrm{R}} = 1$. In simulation, the starting point $i = 1$ and the ending point $i = 5 \times 10^4$ are fixed and the periodic boundary condition is given. All the physical quantities are the international system of unit. The bead displacement is solved by a series of equations of motion of Eq. (1) and the corresponding velocity is obtained as well.

In the following, we will study two kinds of collision between two solitary waves. One is for two same amplitude waves, the other is for two different amplitude waves.

(i) Collision between two same amplitude waves

First, according to Eqs. (7) and (8), the left solitary wave L with the initial data $\varepsilon_{\mathrm{L}} = 0.001$, at the point of the 10^4-th bead, propagates freely from left to right, as shown in Fig. 2. It is observed that the waveform and the propagation velocity remain unchanged during the collision process with the right solitary wave. We compare our numerical results with the analytical one of Eq. (8) and obtain a good agreement between them, as shown in Fig. 3. It indicates that the KdV solitary waves can propagate steadily in the 1D bead chain. Then according to Eqs. (9) and (10), the right solitary wave R with the same initial condition $\varepsilon_{\mathrm{R}} = \varepsilon_{\mathrm{L}} = 0.001$, at the point of the 4×10^4-th bead, propagates freely from right to left. Initially, both solitary waves are far apart. After some time, they interact, collide, and then depart. There are four different cases of colliding: (a) A_+^{L} & A_+^{R}, (b) A_-^{L} & A_-^{R}, (c) A_+^{L} & A_-^{R}, and (d) A_-^{L} & A_+^{R}, where "$+$" and "$-$" represent the propagation direction of solitary wave,[40] shown in Fig. 4. It is clear that after collision, their wave forms still remain unchanged. However, there is an interesting phenomenon that there is no phase shift for both solitary waves compared with those without the collision, as shown in Fig. 5. Figures 5(a)–5(d) show the comparisons between the solitary waves with and without collisions corresponding to Figs. 4(a)–4(d), respectively. The black solid lines stand for solitary waves after collision and the red solid lines are the same solitary waves propagating without collisions. Figure 6 shows the corresponding collision profiles to Fig. 5 for the bead displacements. It is found that there is no phase shift after any collision. This result is interesting since it is different from that found in the nonlinear lattice, in the water waves, in the Bose–Einstein condensations.

(ii) Collisions between two solitary waves with different amplitude

It is found from the above section that the waveform and the propagation velocity of two colliding solitary waves remain unchanged after collision. In this section, we consider

the collision between two solitary waves with different amplitudes. The initial condition of the solitary wave R is given by a small parameter $\varepsilon_{\mathrm{R}} = 0.001$, but the solitary wave L is given by $\varepsilon_{\mathrm{L}} = 0.0015$. The results are shown in Fig. 7. It is noted from Fig. 7 that initial amplitudes of colliding solitary waves L and R are about $A_{\mathrm{L}} = 0.01309$ and $A_{\mathrm{R}} = 0.00582$, respectively. There are four cases. No phase shift is observed for a solitary wave after collision, as shown in Fig. 8. We can also obtain from Fig. 9 corresponding to Fig. 8 that the head-on collision between two opposite propagating KdV solitary waves can pass through each other as if without suffering any interaction. There is no phase shift between them.

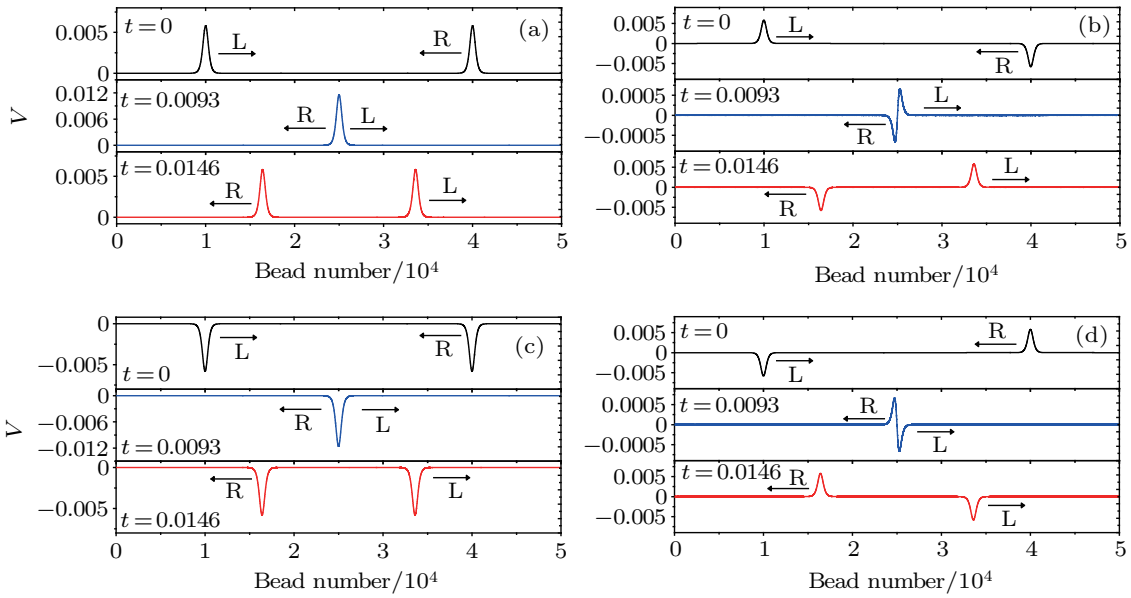


Fig. 4. (color online) The interaction process of head on collision between two solitary waves. Panels (a), (b), (c), and (d) correspond to the four cases. L and R represent the left and right solitary waves, where $A_{\mathrm{L}} = 0.00582$ and $A_{\mathrm{R}} = 0.00582$. The arrows stand for the propagation directions of waves. The black solid line represents the initial state of the solitary waves of L and R, the blue solid line represents the wave profile at the critical point when the maximum amplitude is reached during the collision between two solitary waves. The red solid line represents the evolution of solitary waves L and R after collision. Four different cases are shown in panels (a), (b), (c), and (d). Case (a) is for A_{+}^{L} & A_{+}^{R}, case (b) for A_{-}^{L} & A_{-}^{R}, case (c) for A_{+}^{L} & A_{-}^{R}, and case (d) for A_{-}^{L} & A_{+}^{R}. Here A^{L} and A^{R} represent amplitudes of solitary waves L and R, respectively, while "+" and "−" represent the propagation directions of solitary waves, respectively.

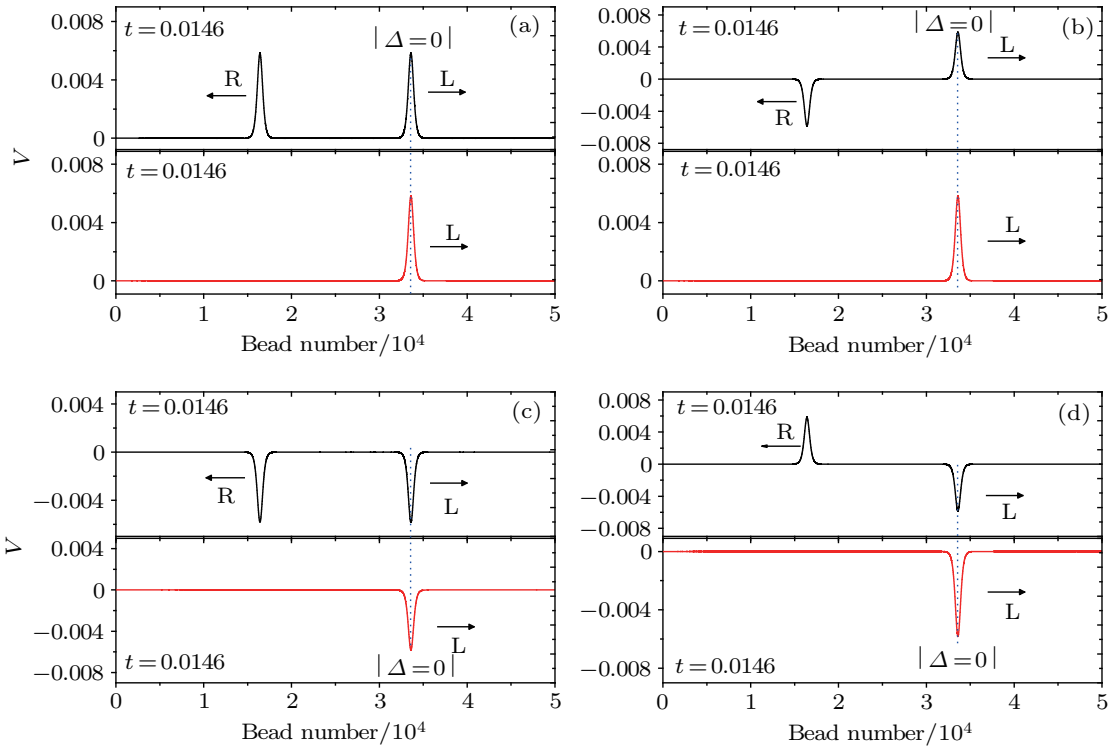


Fig. 5. (color online) The definition of the phase lags of solitary waves. The arrows stand for the propagation directions of waves, the red solid line represents the solitary wave L without collision and the black solid line represents solitary wave L after collision. "Δ" stands for the phase shift.

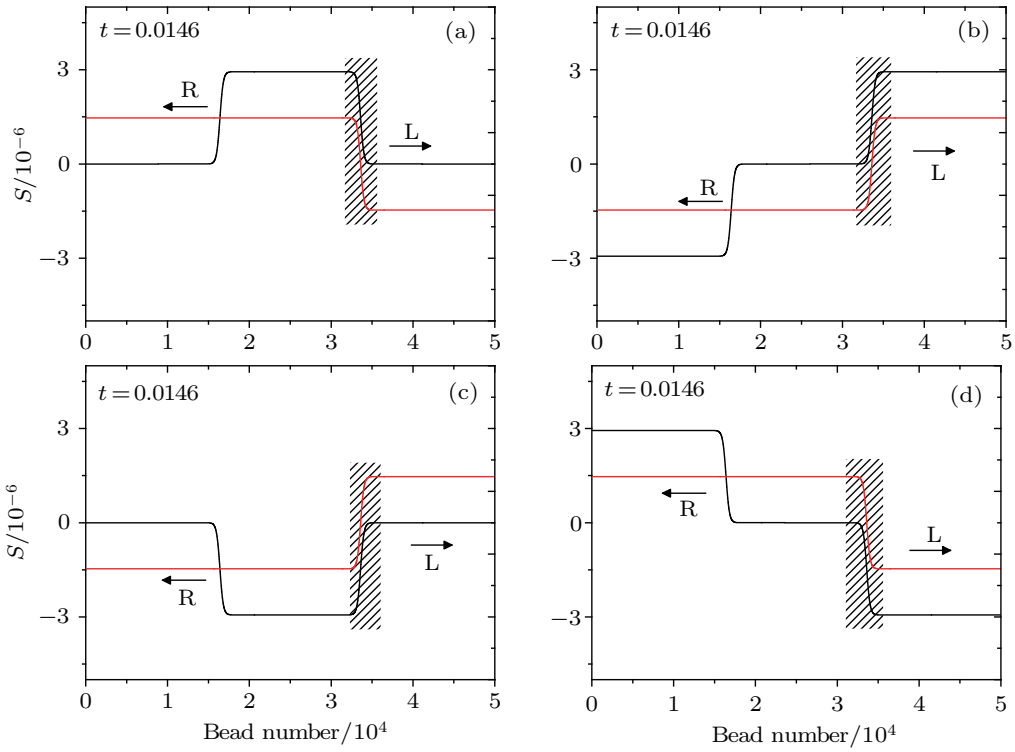


Fig. 6. (color online) Displacement diagram of solitary waves corresponding to Fig. 5. The arrows stand for the propagation directions of waves. The red solid line represents the kink L without collision and the black solid line represents the kink L after collision.

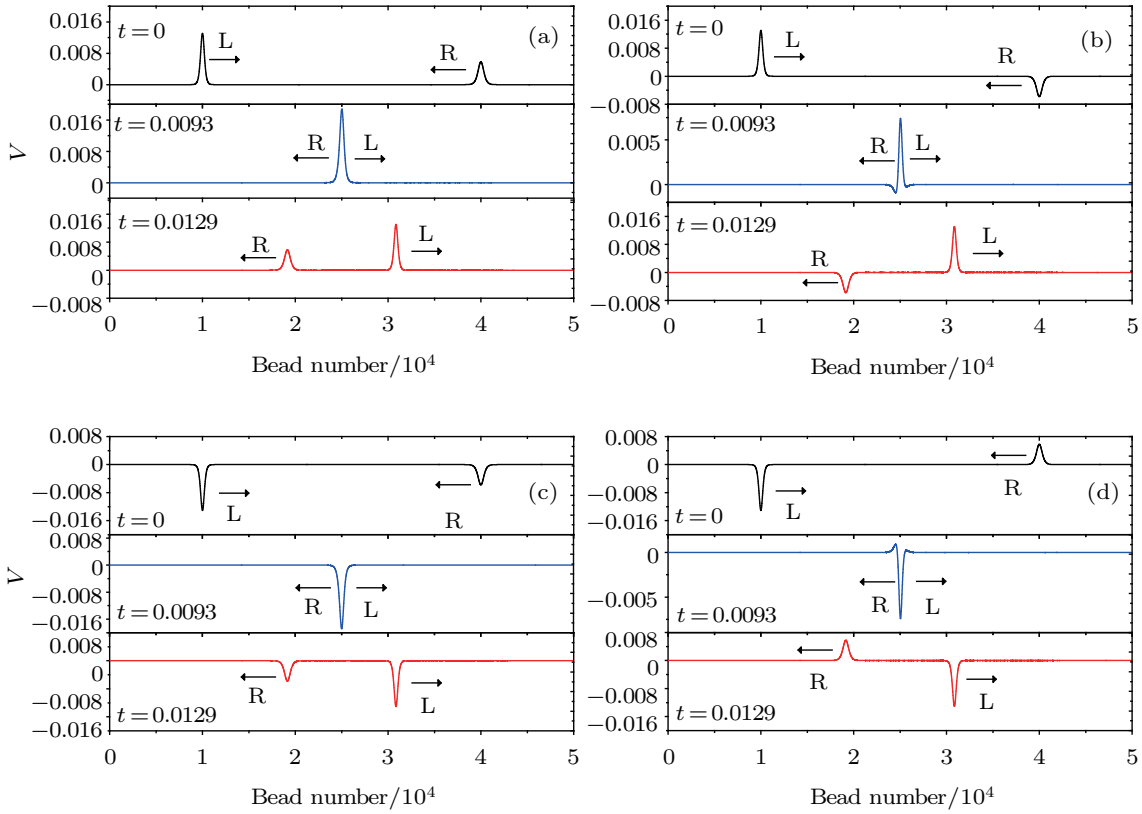


Fig. 7. (color online) The interaction process of the head on collision between two solitary waves L and R. There are four cases. Initial amplitudes of colliding solitary waves L and R are about $A_{\rm L} = 0.01309$ and $A_{\rm R} = 0.00582$, respectively. In the figure, the arrows stand for the propagation directions of waves. The black solid line represents the initial state of the solitary waves L and R, the blue solid line represents the collision of solitary waves L and R and the red solid line represents the evolution of solitary wave L and R at the different times after collision. Four different cases are shown in panels (a), (b), (c), and (d). Case (a) is for $A^{\rm L}_{+}$ & $A^{\rm R}_{+}$, case (b) for $A^{\rm L}_{-}$ & $A^{\rm R}_{-}$, case (c) for $A^{\rm L}_{+}$ & $A^{\rm R}_{-}$, and case (d) for $A^{\rm L}_{-}$ & $A^{\rm R}_{+}$. Here $A^{\rm L}$ and $A^{\rm R}$ represent amplitudes of solitary waves L and R, respectively, while "+" and "−" represent the propagation directions of solitary waves, respectively.

The maximum amplitude in the process of interaction between two solitary waves is also studied, as shown in Fig. 10. Comparisons are given among three results. It should be noted here that there is no obvious boundary among the numerical results, the linear result of $A = A^{\mathrm{L}} + A^{\mathrm{R}}$ where $A^{\mathrm{L}} = \varepsilon s^{\mathrm{L}}$ and $A^{\mathrm{R}} = \varepsilon s^{\mathrm{R}}$, and the modified result $A^{\mathrm{L}} + A^{\mathrm{R}} + \varepsilon s_1$ for the different velocity solitary waves. Good agreements among them are observed. However, small differences are observed when the colliding solitary wave is large. For further investigation, figure 11 also shows the dependence of the maximum amplitude during the colliding process on the amplitudes of two colliding solitary waves. It is obviously noted that the maximum amplitude in the colliding process increases as the two amplitudes of the colliding solitary waves increase.

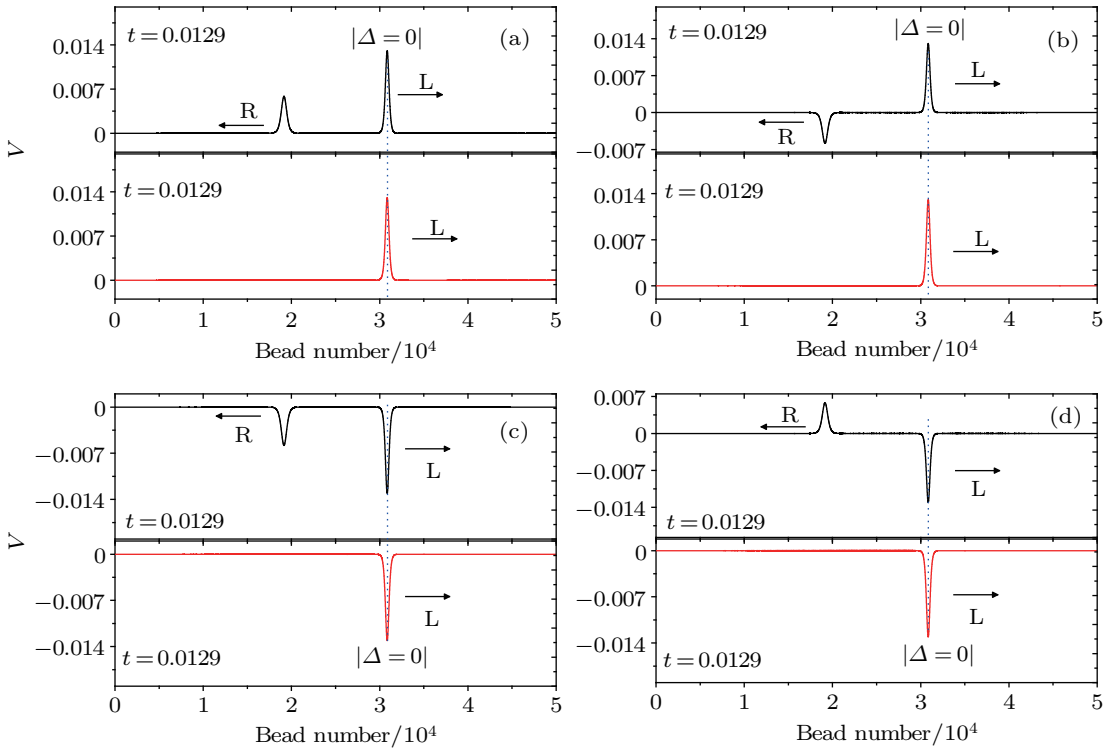


Fig. 8. (color online) The definition of the phase lags of both solitary waves. In the figure, the arrows stand for the propagation directions of waves. The red solid line represents the solitary wave L without collision and the black solid line represents solitary wave L after collision. "Δ" stands for the phase.

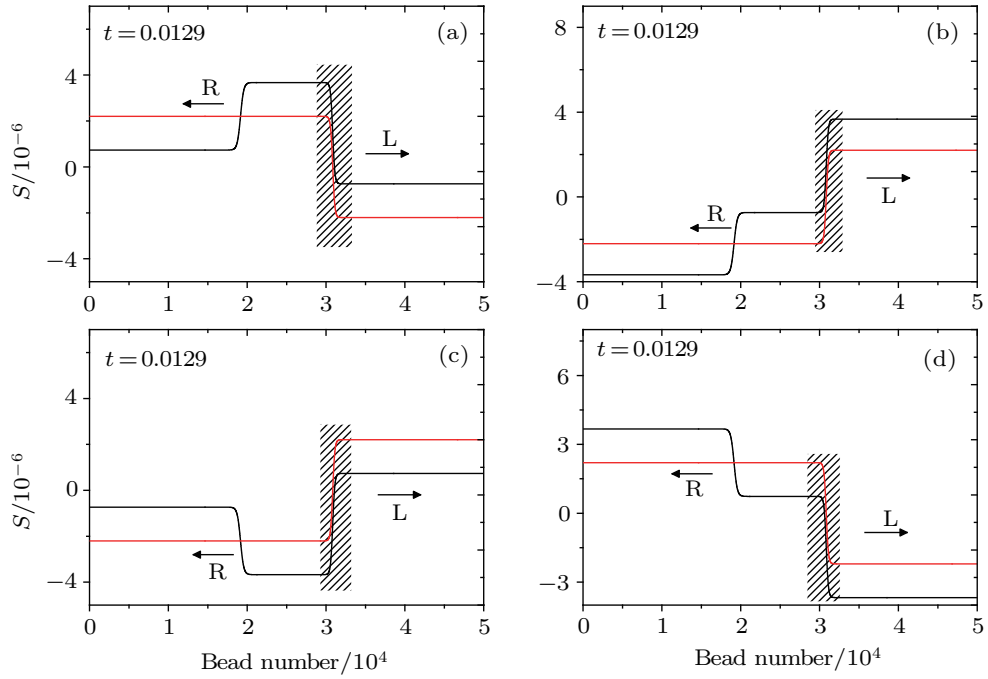


Fig. 9. (color online) Displacement diagram of solitary waves corresponding to Fig. 8. The arrows stand for the propagation directions of waves. The red solid line represents the kink L without collision and the black solid line represents the kink L after collision.

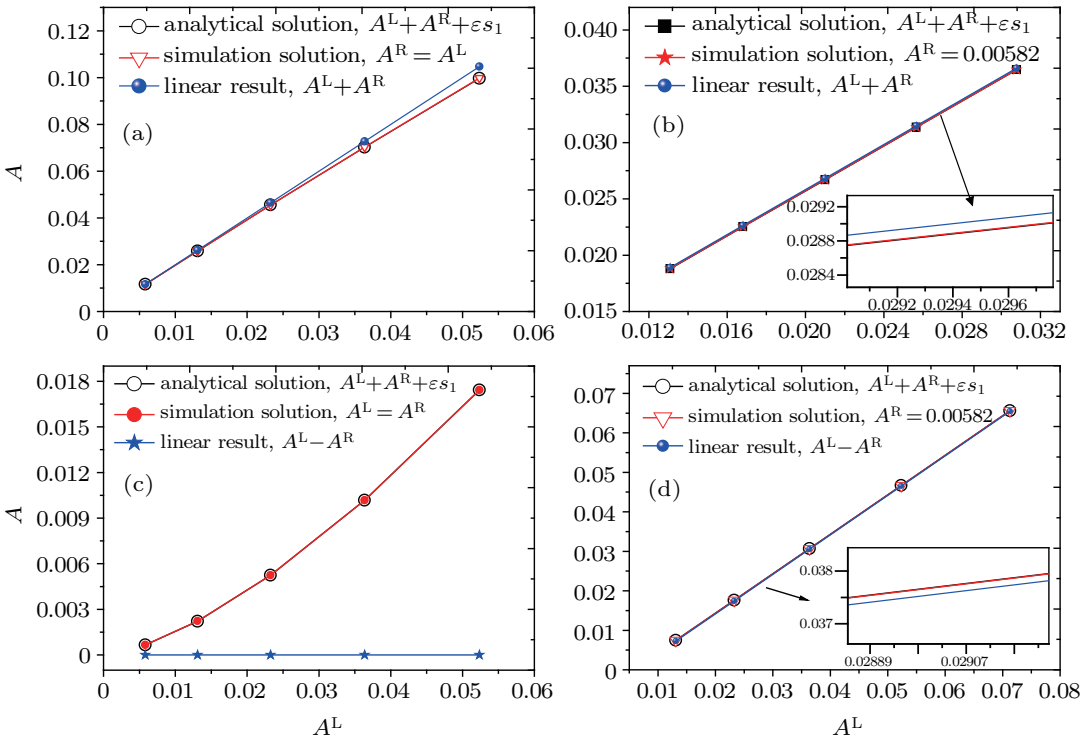


Fig. 10. (color online) The maximum amplitude in the colliding processes as a function of the amplitude of the solitary wave L. Panels (a) and (c) corresponding to $A^L = A^R$, but the amplitude of the solitary wave R is fixed in panels (b) and (d). The red dots are from the numerical results, the black ones are the analytical results by further considering the higher order terms of $O(\varepsilon)$, $A^L + A^R + O(\varepsilon)$, the blue ones are the linear results of $A^L + A^R$, where A^L and A^R are the amplitudes of solitary waves L and R, respectively.

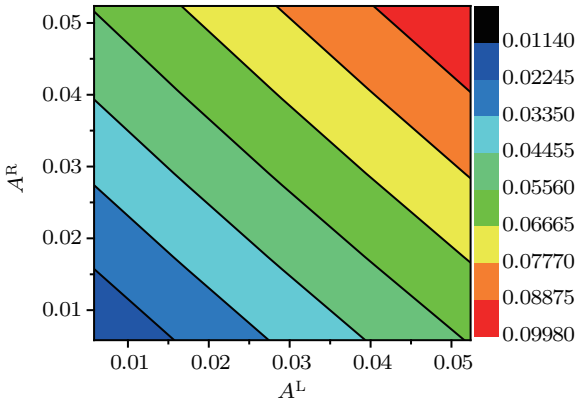


Fig. 11. (color online) The dependence of the maximum amplitude in the colliding processes on both amplitudes (A^L, A^R) of the two colliding solitary waves L and R.

4. Conlusions

In this paper, we have studied the head on collision between two opposite propagating solitary waves. By using the PLK method, KdV equations are obtained before and after collisions. At the same time, a numerical investigation is given for the head on collision between two KdV solitary waves. The interesting result is that no phase shift is observed which is different from that found in other branches of physics, such as in plasma physics, fluid dynamics, Bose–Einstein condensation, solid physics, and optics. The maximum amplitude during the head on collision between two solitary waves in a 1D bead chain is also studied. It is found that it is almost equal to the linear sum of the amplitudes of two solitary waves. It is in good agreement between them when the amplitudes of the two colliding solitary waves are small enough, while the difference increases as the amplitudes of both colliding solitary waves increase.

References

[1] Korteweg D J and Vries G D 1895 *Philosophical Magazine* **39** 422
[2] Zabusky N J and Kruskal M D 1965 *Phys. Rev. Lett.* **15** 240
[3] Nesterenko V F 1983 *J. Appl. Mech. Tech. Phys.* **24** 733
[4] Coste C, Falcon E and Fauve S 1997 *Phys. Rev. E.* **56** 6104
[5] Nesterenko V F 2001 *Dynamics of Heterogeneous Materials* (New York: Springer)
[6] Lazaridi A N and Nesterenko V F 1985 *J. Appl. Mech. Tech. Phys.* **26** 405
[7] Su C H and Mirie R M 1980 *J. Fluid Mech.* **98** 509
[8] Gardner C S, Greene J M, Kruskal M D and Miura R M 1967 *Phys. Rev. Lett.* **19** 1095
[9] Huang G X and Velarde M G 1995 *Phys. Rev. E* **53** 2988
[10] Xu Y X, Liu Z M, Lin M M, Shi Y R, Chen J M and Duan W S 2011 *Phys. Plasmas* **18** 052301
[11] Han J N, Du S L and Duan W S 2008 *Phys. Plasmas* **15** 112104
[12] Li S C and Duan W S 2008 *Eur. Phys. J. B* **62** 485
[13] Zhang Y and Ding N 2008 *Chin. Phys. B* **17** 2994
[14] Nejoh Y 1992 *Phys. Fluids B: Plasma Physics* **4** 2830
[15] Sokolow A and Sen S 2005 *Phys. Rev. Lett.* **94** 178002
[16] Nesterenko V F, Daraio C, Herbold E B and Jin S 2005 *Phys. Rev. Lett.* **95** 158702
[17] Job S, Melo F, Sokolow A and Sen S 2007 *Granular Matter* **10** 13
[18] Harbola U, Rosas A, Romero A H, Esposito M and Lindenberg K 2009 *Phys. Rev. E* **80** 051302
[19] Harbola U, Rosas A, Romero A H and Lindenberg K 2010 *Phys. Rev. E* **82** 011306
[20] Melo F, Job S, Santibanez F and Tapia F 2006 *Phys. Rev. E* **73** 041305
[21] Doney R L 2005 *Phys. Rev. E* **72** 041304

[22] Boechler N, Theocharis G, Job S, Kevrekidis P G, Porter M A and Daraio C 2010 *Phys. Rev. Lett.* **104** 244302
[23] Theocharis G, Boechler N, Kevrekidis P G, Job S, Porter M A and Daraio C 2010 *Phys. Rev. E* **82** 056604
[24] Job S, Santibanez F, Tapia F and Melo F 2009 *Phys. Rev. E* **80** 025602
[25] Martinez A J, Yasuda H, Kim E, Kevrekidis P G, Porter M A and Yang J 2016 *Phys. Rev. E* **93** 052224
[26] Li F, Zhao L X, Tian Z H, Yu L Y and Yang J 2013 *Smart Mater. Struct.* **22** 035016
[27] Liu S W, Yang Y Y, Duan W S and Yang L 2015 *Phys. Rev. E* **92** 013202
[28] Shen Y, Kevrekidis P G, Sen S and Hoffman A 2014 *Phys. Rev. E* **90** 022905
[29] Qi X, Xu Y X, Duan W S, Zhang L Y and Yang L 2014 *Phys. Plasmas* **21** 082118
[30] Zhang J, Yang Y, Xu Y X, Yang L, Qi X and Duan W S 2014 *Phys. Plasmas* **21** 103706
[31] Jaiswal S, Bandyopadhyay P and Sen A 2014 *Phys. Plasmas* **21** 053701
[32] Roy K, Chatterjee P and Roychoudhury R 2014 *Phys. Plasmas* **21** 104509
[33] Maxworthy T 1976 *J. Fluid Mech.* **76** 177
[34] Sharma S K, Boruah A and Bailung H 2014 *Phys. Rev. E* **89** 013110
[35] Santibanez F, Munoz R, Caussarieu A, Job S and Melo F 2011 *Phys. Rev. E* **84** 026604
[36] Hinch E J and Saint-Jean S 1999 *Proc. R. Soc. Lond. A* **455** 3201
[37] Spence D A 1968 *Proc. Roy. Soc. A* **305** 55
[38] Leblond H 2008 *J. Phys. B: At. Mol. Opt. Phys.* **41** 043001
[39] Taniuti T and WEI C C 1968 *J. Phys. Soc. Jpn.* **24** 941
[40] Yang Y Y, Liu S W, Yang Q, Zhang Z B, Duan W S and Yang L 2016 *AIP Adv.* **6** 075317
[41] Takato Y and Sen S 2012 *Europhys. Lett.* **100** 24003